

Iterative Extremum Seeking Trim Control on a High Speed Craft by Using Extended Kalman Filter

M. Ertogan

Maritime Faculty-Marine Engineering, Istanbul Technical University, Turkey, ertogan@itu.edu.tr

P.A. Wilson

Faculty of Engineering and the Environment, University of Southampton, U.K., philip.wilson@soton.ac.uk

G. T. Tayyar

Naval Architecture and Marine Engineering, Istanbul Technical University, Turkey, tayyargo@itu.edu.tr

S. Ertugrul

Mechanical Engineering, Istanbul Technical University, Turkey, seniz@itu.edu.tr

ABSTRACT: An automatic trim control of a high-speed craft can decrease fuel consumption. Also, it can increase the safety and comfort of passengers in high-speed craft. This controller can be applied on any interceptor, trim tabs, sterndrive propulsion unit, etc. An iterative extremum seeking trim control of a high-speed craft is currently being studied in this project. Hence, a pair of interceptors and trim tabs were mounted on the high-speed craft Volcano 71, with a length 10.86m for obtaining sea trials' data and real-time applications in real sea conditions. The sterndrive engines of Volcano 71 have engines rated at 2x385 HP, and it reaches a top speed of 40 knots. The pulse width modulation (PWM) drivers were provided for the interceptor and trim tab systems and operated in open loop control. A Global Positioning System (GPS) and an Attitude and Heading Reference System (AHRS) were used to collect feedback data in changing sea conditions for system identification and to measure maximum effects. The GPS will be utilized as sole sensor for final prototype. Then, an iterative extremum seeking trim control of the craft studied on a coupled identification nonlinear model by using an Extended Kalman Filter (EKF) algorithm. Successful results were achieved with EKF controller in calm sea conditions. The design of the automatic trim control is currently underway going on for little wavy sea conditions and/or variable ship speeds. After finalizing the simulation studies of the iterative extremum trim control on the nonlinear model, full scale trials will be realized. The performance of the automatic trim control for a high-speed craft can be evaluated by the speed value at the same motor power while a trim tab, an interceptor, and/or sterndrive system are either active or off.

1 INTRODUCTION

The maintaining of the optimal trim angle for a high-speed craft using the trim tab, the interceptor, or marine propulsion unit systems, under changing sea conditions provides the increment on its speed, energy efficiency, and well sight during a captain's driving.

The last arrangement of trim tab actuator for power boats was patented see (Cotton, 2000). The interceptor design arrangement for dynamic trim control was worked and patented (Olofsson, 2014). In addition to these works, in the literature, design of the trim tuning actuators, and necessary forces on a high-speed craft were studied in a lot of papers.

The empirical equations were studied to calculate pressure and resistance forces at different trim angles for a triangular and rectangular planning forms (Payne, 1990). The effect of trim tab, interceptor, and integrated interceptor with trim tab systems on resistance reduction were examined (Tsai, and Hwang, 2004). Wave loads on a high-speed catamaran equipped with active trim tabs were measured, hence between computed and measured unsteady bending moments were compared, and good agreement was found for bow quartering seas (Davis et al., 2004). An experimental study of interceptors for drag reduction of sailing yachts was done (Day, and Cooper, 2011). The other experimental studies on

interceptor's effectiveness on high-speed planning crafts were realized (Karimi et al., 2013; Kwang-Cheol et al., 2013).

The automatic optimal control methods for tuning the dynamic trim of a high-speed craft have not studied enough in the articles. However, there are few patents on the dynamic trim control of a high-speed craft. In one of the patents, the angle of trim of a sterndrive propulsion unit is controlled according to a referenced trim angle of a high-speed craft or when the acceleration of the hull exceeds a predetermined value (Funami, and Watanabe, 1992). In the other patented work, the trim tab system are moved according to a predetermined speed by stages (Davis, 1993). In another patented work, the craft is trimmed up as long as the cruising speed continues to increase by using the marine propulsion unit, then it is trimmed down during the cruising speed slowing down so as to maintain the highest speed possible for under running condition (Uenage, and Hirano, 1994). In the recent patented work, multiple trim positions are selected through the course of operation in the defined mode such as normal mode etc. Each selected trim position, an operation speed is measured, and compared the stored data. So, the current operational mode parameter is defined, and then trim position is selected. This application is like look-up table control method (Krueger, 2002).

In the literature, there are a variety of optimal control methods studied for general engineering problems. However, the peak seeking control application on flight performance was found in the literature for the close working to the optimal trim control of a high-speed craft. The peak seeking control was used to form flight for drag reduction, and tuning a wing angle. The optimal control includes a time varying Kalman Filter and a Newton-Raphson algorithm (Ryan, and Speyer, 2010, 2013; Ryan, 2012). Also, this peak-seeking control method was studied for real-time trim optimization for reduced fuel consumption of an airplane by researchers at the National Aeronautics and Space Administration (NASA) Dryden Flight Research Center. In real-time application, deflections of symmetric ailerons, trailing-edge flaps, and leading-edge flaps of the airplane were controlled by using the Kalman Filter with a Newton Raphson algorithm for aiming optimization of fuel flow (Brown, and Schaefer, 2013). In addition to these applications, the extremum seeking control technique was used to control a

variable pitch propeller angle of a turboprop engine (Cazenave, T.J.W., 2012).

In this optimal trim control application project, a pair of interceptors and trim tabs were mounted on the Volcano71, in length 10.86m for obtaining sea trials' data for obtaining model and real-time applications in real sea conditions. The nonlinear coupled mathematical model of a high-speed-craft equipped with the trim tab/interceptor systems was studied to design advanced optimal trim controller, and presented in the paper (Ertogan et al., 2017). In this paper, the designing automatic trim control, and the application results were explained by given summary of test-setup, sea-trials, and modelling.

2 A TEST SYSTEM SET-UP, SEA TRIALS AND NONLINEAR MODELLING OF A HIGH-SPEED CRAFT EQUIPPED WITH INTERCEPTOR/TRIM TAB SYSTEMS

2.1 Test system set-up, manual control test results of interceptor/trim tab systems

Volcano 71 is a high-speed craft with a deep V form. Its profile view is given in Figure 1. The interceptor, and the trim tab systems were installed for the real-time applications, as shown in Figure 2. The trim of the sterndrive propulsion systems of the gasoline engines can be manually controlled by a hydraulic assisted system. These manual systems will be controlled by an algorithm when the trim system becomes automatic.



Figure 1. The high-speed craft, Volcano 71, in length 10.86m.



Figure 2. The pair of interceptors and trim tabs were mounted on the high-speed craft, Volcano 71 having sterndrive propulsion system unit.

The other particulars of Volcano 71 are as follows: length overall LOA=10.86m, length on the waterline LWL=9.4m, beam B=3.3 m, depth D=1.15 m, deadrise angle $\beta=16^\circ$. Hydrostatic characteristics of it are displacement $\Delta=5.35$ tons, draft T=0.45 m, metacentric height $\overline{GM}=0.64$ m. Volcano71 has a 2x385 BHP sterndrive twin engine reaching a speed up to 40 knots with the installed propellers.

The blade size and stroke of the interceptor's are 430mm, and 50mm, respectively. The size of the trim tab's plate of the each engine is 450mm x 250mm. The Pulse Width Modulation (PWM) drivers were provided for the interceptor, trim tab systems, and sterndrive systems.

An AHRS, including tri-axial accelerometer, gyroscope, magnetometer, was chosen to measure the ship's 3-axis rotational and linear motions. The measurement range of the AHRS's outputs are ± 4 g with 12-bit reading per axis, and $\pm 250^\circ/s$ with 16-bit reading per axis. Also, a GPS was used, and its data output rate is 1 Hz to 10 Hz. The GPS and the AHRS have been used for data acquisition for modelling, and designing the controller. The GPS was utilized and considered as sole sensor for final prototype.

The data was collected from sea trials in Tuzla, Istanbul in order to obtain a coupled pitch and surge dynamic model. In the sea trials, the interceptor/trim tab systems were opened, and closed gradually during a constant motor power, and this operation was repeated at variable motor power. So, the experimental data was collected from the sensors under environmental conditions.

A sample of the trim tab system's operation at approx. 2700 motor rpm is shown on Figure 3. The maximum motor boat's speed is reached during the trim tab position at 60%, and at approx. 2700 motor rpm for this application.

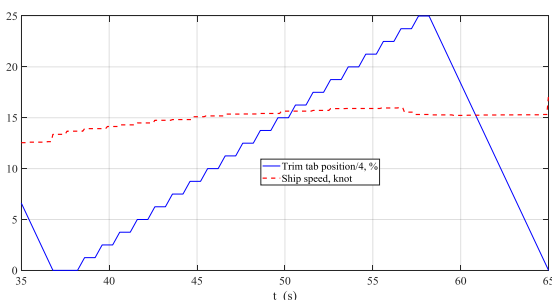


Figure 3. The craft's speed at approx. 2700 motor rpm, under condition the trim tab system's movement.

In the following operation, the trim tab position was kept at 60% for the same motor power, and the motor boat's speed data was measured. This operation is illustrated on Figure 4.

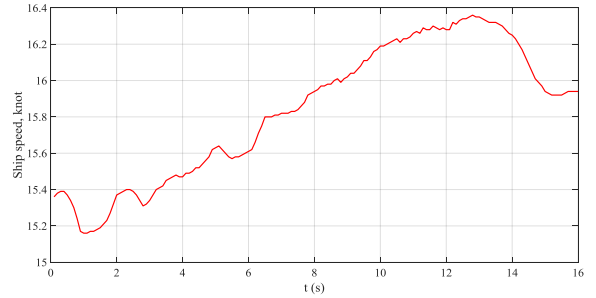


Figure 4. The craft's speed at approx. 2700 motor rpm during the trim tab position at 60%.

However, an optimal trim position is varied as an environmental condition change for a constant motor power. So, the trim tab/interceptor system operations were repeated under changing environmental conditions, and the sea trial data was collected to model of the craft. Hence, the optimal trim control design can be done on the nonlinear coupled model.

2.2 A nonlinear coupled model of a high-speed craft with interceptor/trim tab systems

Artificial Neural Networks (ANN), with the ability to learn complicated relations from Multi-Input and Multi-Output (MIMO) imprecise data, can be utilized to model non-linear coupled system dynamics. ANN should be applied because of its advantages. These advantages are to learn, and generalize from training data. In addition to these, it estimates from the given imprecise data, and makes associations between the training data and the validation data (Hagan et al., 2014; Demuth et al., 2013). The ANN model was used for the nonlinear coupled speed and pitch angle variables, and its structure is illustrated Figure 5.

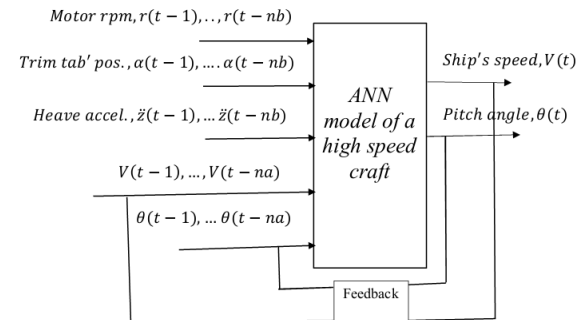


Figure 5. The Artificial Neural Network (ANN) model of the craft, based on sea trial data.

In this figure, n_a represents the past values' number of the outputs as a ship speed signal V , a pitch motion angle signal θ° , and n_b stands for the past values' number of the inputs as an engine speed signal r , a trim tabs/interceptor' position signal α , a heave acceleration signal \ddot{z} . The sampling time as Δt was taken 0.1 s in the applications. The input and output signals are scaled to the interval [-1, 1].

In the Extended Kalman Filter (EKF) extremum seeking trim control application, the ANN model for the sea state 2 condition (Ertogan et al., 2017) was used. The input sea trial data for the ANN model is given on Figure 6.

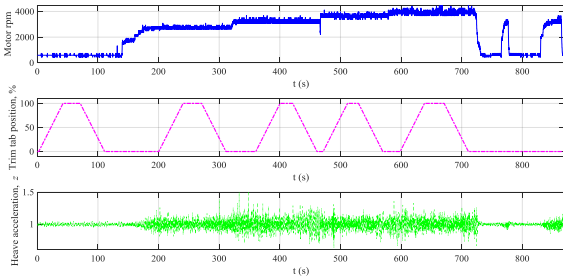


Figure 6. The sample input data for the ANN model

The ANN model consists of two hidden layers. The neurons' number of the first, and the second hidden layers are 5, and 4, respectively. This ANN model was trained by the Levenberg-Marquardt algorithm. $n_a = 7$, $n_b = 5$ were selected, so 29 inputs, and 2 outputs ANN model was used. The log-sigmoid activation function was used for both of the hidden layers. The converging output data between the experimental data and the ANN model output data for the pitch motion angle, θ° and the craft's speed, knot, are shown on Figure 7.

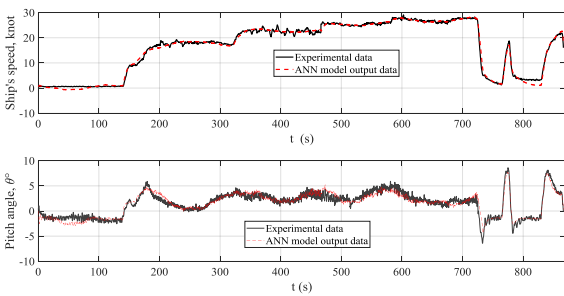


Figure 7: The comparison between the experimental data and the ANN model output data for the pitch motion, and the high-speed craft's speed.

3 THE EXTREMUM SEEKING CONTROL WITH AN EXTENDED KALMAN FILTER CONTROL ALGORITHM

3.1 The Extremum Seeking Control

The aim of the iteratively extremum seeking control to lead the position, $\alpha(t)$, of a system to obtain the maximum performance function, $V(\alpha(t))$. The extremum seeking closed-loop control block diagram is shown in Figure 8. In this control block diagram, $\alpha(t)$ is one of the states of the system. The performance function magnitude have an effect on the system dynamics. The calculated differences are used to estimate the current gradient, g_t , and the Hessian, H_t for the time varying Extended Kalman Filter (EKF) method with a Newton Raphson algorithm. Hence, the position command is calculated by combining the gradient, Hessian, and gain, K , $\alpha_t = Kb_t H_t^{-1}$ to drive the system lead the maximum performance (Ryan, and Speyer, 2010, 2013; Ryan, 2012).

A filter is used to reduce the noise. In addition to this, the position command should be calibrated according to the actuator driver input range. A persistent excitation signal (PE) is added to the smoothed position command to observe the performance function. The EKF control method uses position, and performance function measurements directly to estimate the gradient, and the Hessian. The estimation method may be used to solve many engineering problems.

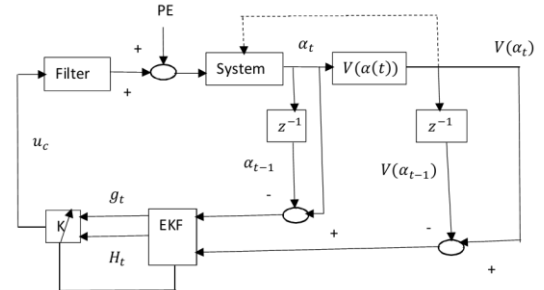


Figure 8. An iteratively extremum seeking control block diagram (Ryan, and Speyer, 2010).

3.2 The Extended Kalman Filter control algorithm

The Extended Kalman Filter (EKF) algorithm is used for an extremum seeking control (Ryan & Speyer 2010, 2013). Objective function including the gradient and the Hessian is predicted with a linear time varying EKF. A Taylor series expansion of an objective function $V(\alpha)$ around α_t , includes first and second order terms is given in (1). g_{α_t} is the gradient at α_t , H_{α_t} is the Hessian at α_t , $o(\cdot)$ represents higher order terms.

$$V(\alpha) \cong V(\alpha_t) + g_{\alpha_t}(\alpha - \alpha_t) + \left(\frac{1}{2}\right) H_{\alpha_t}(\alpha - \alpha_t)^2 + o(\alpha - \alpha_t) \quad (1)$$

Evaluating (1) at α_{t-1} and rearranging leads to

$$\delta V_t = g_t \delta \alpha_t + \left(\frac{1}{2}\right) H_t \delta \alpha_t^2 \quad (2)$$

where $\delta V_t = V_t - V_{t-1}$ and $\delta \alpha_t = \alpha_t - \alpha_{t-1}$. The higher order terms are dropped, so the objective function is adequately modelled as a quadratic function at any particular position. The discrete time equation of the objective function presents the states of the system. The estimation state vector is given (3).

$$\hat{x}_t = [\hat{g}_t \hat{H}_t]^T \quad (3)$$

Taking N sample measurements lead to improve the estimation accuracy, at each iteration t . But, more samples cause a slower convergence. The N sample measured vector of the output/outputs variables of the objective function is written in (4).

$$\delta V_t = \begin{bmatrix} V(\alpha_t) - V(\alpha_{t-1}) \\ \vdots \\ V(\alpha_t) - V(\alpha_{t-N}) \end{bmatrix} \quad (4)$$

A persistent excitation (PE) signal may be added to the smoothed position command to ensure observability of the objective function. If PE signal is added, a certain number of excitation points α_s can be added to the measured vector. The measurement matrix of the state/states of the objective function is given in (5), according to the Taylor series approximation.

$$M_t = \begin{bmatrix} \alpha_t - \alpha_{t-1} & \left(\frac{1}{2}\right)(\alpha_t - \alpha_{t-1})^2 \\ \vdots & \vdots \\ \alpha_t - \alpha_{t-N} & \left(\frac{1}{2}\right)(\alpha_t - \alpha_{t-N})^2 \end{bmatrix} \quad [5]$$

The measurement equation of EKF to take form

$$\delta V_t = M_t x_t + v_t \quad (6)$$

v_t is the Gaussian measurement noise of variance R_t , and x_t is a 2 x 1 vector representing the derivative parameters to estimate. Evaluating at the next time step with a change of $\delta \alpha_t$ in a state provides (7) as taking the Taylor series expansion of the derivatives term.

$$\begin{aligned} V_{t+1} &= \dot{V}_t + (\alpha_t - \alpha_{t-1}) \ddot{V}_t \\ V_{t+1} &= \ddot{V}_t \end{aligned} \quad (7)$$

The discrete state matrix presents the derivatives dynamics, and it is given in (8).

$$A_t = \begin{bmatrix} 1 & \alpha_t - \alpha_{t-1} \\ 0 & 1 \end{bmatrix} \quad (8)$$

If the number of derivatives taken into account in the Taylor expansion is increased, it would cause more computation, and stop making sense after a certain order.

The discrete time process of the derivatives behaviour is given in (9), where w_t is the Gaussian process noise with variance Q_t .

$$x_{t+1} = A_t x_t + w_t \quad (9)$$

A priori error covariance matrix P_t^- is computed as follows;

$$P_t^- = A_t P_{t-1} A_t^T + W_t Q_{t-1} W_t^T \quad (10)$$

Where, W_t represents the jacobian matrix of the state transition model with respect the process noise w_t . EKF equations for estimation of the derivatives are written in (11). Detailed explanations of EKF can be found in (Brown & Hwang 1997; Grewal & Andrews 2001)

$$\begin{aligned} K_t &= P_t^- M_t^T (M_t P_t^- M_t^T + R_t)^{-1} \\ \hat{x}_t &= \hat{x}_t^- + K_t (\delta V_t - M_t \hat{x}_{t+1}^-) \\ P_t &= (I - K_t M_t) P_t^- (I - K_t M_t)^T + K_t R K_t^T \end{aligned} \quad (11)$$

4 AN ITERATIVE EXTREMUM SEEKING TRIM CONTROL OF A HIGH-SPEED CRAFT BY USING INTERCEPTOR/TRIM TAB SYSTEMS

4.1 Applications of EKF on extremum seeking trim control of a high-speed craft nonlinear coupled model

The EKF iteratively extremum seeking trim control was applied on the nonlinear coupled ANN model (ANNM) of a high-speed craft by using the interceptor/trim tab systems, shown in Figure 9. In this closed-loop control, α_n is the interceptor/trim tab systems' position, %, as a state variable, $V(\alpha_n)$ is the high-speed craft's speed, knot, as an objective function output. Indices, n indicates the number of closed-loop. delay time was used to observe the response of the interceptor/trim tab systems' position in changing environmental condition. In this control application, delay time was taken as 10 s. \hat{g}_n is the estimation of the gradient value, and \hat{H}_n is the estimation of the Hessian value in each closed-loop. The persistent excitation (PE) signal

was not needed, because the mathematical model is based on sea trial data including continuously changing variables. The sea trial data consists of pitch motion, θ° heave acceleration, \ddot{z} , cruise speed, V , motor rpm, and the interceptor/trim tab systems' position, α .

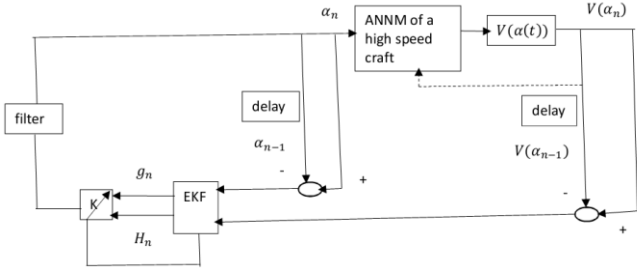


Figure 9. EKF extremum seeking trim control closed-loop block diagram on the ANN model of the high-speed craft.

The input-output schema of the ANN model of a high-speed craft is given in Figure 10. In this application, the sample time was taken as 0.1 s. So, z^{-1} was defined 0.1 s delay during running of the ANN. For each simulation, motor rpm was taken as constant. Also, the interceptor/trim tab systems' position, α_n was used as constant in each closed-loop for the input of the ANN model. nb_{in} , na_{out} were defined as 5, and 7, respectively for the input of the model.

It was aimed in these control design application that the interceptor/trim tab systems' position would maintain the optimum position at constant motor power in changing conditions, so a high-speed craft would have maximum speed. The interceptor/trim tab systems' position, $\alpha_n = \alpha_{n-1} + K \frac{\hat{g}_n}{\hat{H}_n}$, was calculated in each closed-loop.

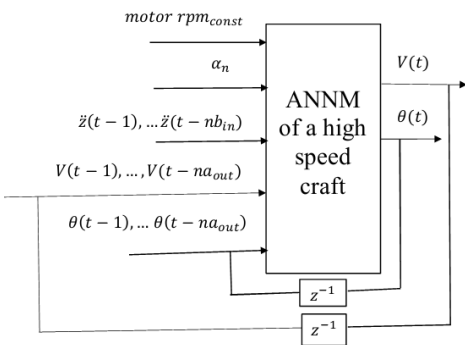


Figure 10. The input-output of the ANN model of a high-speed craft during application of EKF extremum seeking trim control.

As the system approached to the optimum, α_n a trim tab/interceptor systems' position signal became

unstable because of only the Hessian approached to nearly zero value in the gradient and Hessian estimation values. In this situation, the Newton-Raphson method was used. Using the estimates of the actuators' position, the Newton method was carried on (12).

$$\alpha_n = \alpha_{n-1} + \delta \frac{\hat{g}_n}{\hat{H}_n} \quad (12)$$

Where \hat{g}_n and \hat{H}_n are the gradient and the Hessian estimation for the actuators' position at α_{n-1} . δ is fading coefficient based on the standard deviation of the set of the previously commanded the actuators' position signals.

$$\delta = \gamma \frac{1}{n-l} \sum_{i=n-l}^n (\alpha_i - \mu)^2 \quad (13)$$

Where γ is tuning parameter, μ is the mean and l is used to determine the size of the set. As the actuators' position is converging to the optimal value, the fading coefficient δ decreases, since the standard deviation of the previously calculated the actuators' position values is decreasing. Hence, when getting closer to the optimal value, small changes would occur.

4.2 Simulation results

First of all, the EKF extremum seeking trim control was applied by using the sample I, and II objective functions respectively, shown in Figure 11. The objective functions were obtained from sea trial data. The trim tab system was opened and closed gradually by manual control for two different motor power conditions, and collected data the command position signal, and GPS' feedback signal. The objective functions' equations were calculated with the curve fitting method according to the collecting data as the actuators' position, %, and the high-speed craft's speed, knot. It was aimed to check the EKF control algorithm whether working properly, or not in this sample application.

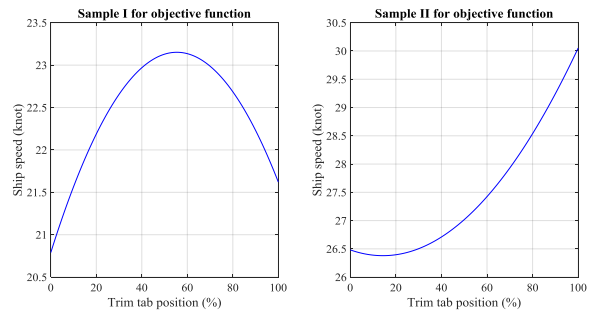


Figure 11. The objection functions, as sample I and II based on the trim tab position, %, and the craft's speed were applied respectively for the EKF extremum seeking control.

In the two consecutive sample I, and II objective functions' application, the trim tab positions were calculated accurately as approximately 60% for the sample I, 80% for the sample II. This sample application results are shown on Figure 12, and 13. In the EKF control sample application, a PE may be needed to calculate the trim tab system's position signal for a long time simulation process, because the objective functions are smooth.

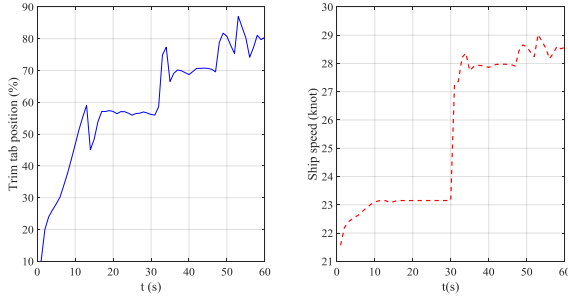


Figure 12. The trim tab positions, %, and the craft's speed, knot, are given by the time axes in consequence of the sample control application.

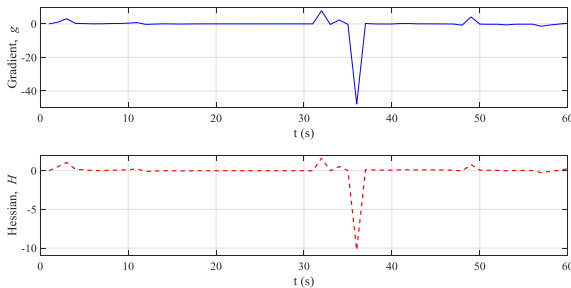


Figure 13. The gradient, and Hessian are shown by the time axes in consequence of the sample control application.

After the EKF extremum seeking trim control was validated, the simulation process was carried out with the ANN model. The EKF control was applied on the ANN model for three different motor rpm as 2600, 3000, and 3700 during changing dynamic conditions such as pitch angle, θ° , heave acceleration, \ddot{z} , etc. The actuators' position, and the high-speed carft's speed values were scaled between 0-1, while the gradient and Hessian estimation values were calculated. The control gain, K , was needed to tune between 0.280-0.285 during switching 2600-3700 motor rpm. Also, the Newton method was used to calculate the trim tab system's position signal.

As a result of these applications, the EKF extremum seeking control was lead to maintain the optimum position of the trim tab systems's position, so the optimum speed values were obtained. Also, the pitch motions were nearly reduced because of the

optimum trim condition. The results of these control applications are given on Figures 14-22. The highest speed increase with optimum trim condition was obtained for the semi-planing running regime of the high-speed craft.

However, this extremum seeking control method takes time to lead to the the optimum trim condition. Also, the control gain, K , needs to be tuned during changing motor power. So, the EKF extremum seeking trim control should be used with the aid of an advanced tuning method.

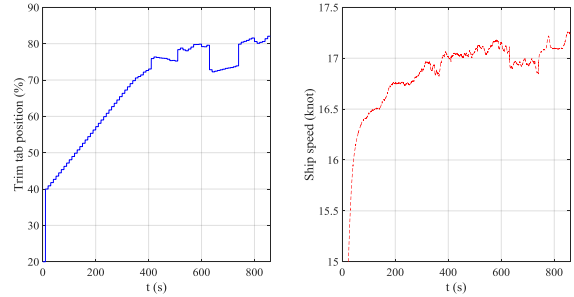


Figure 14. The trim tab positions, %, and the craft's speed, knot, are given by the time axes in consequence of the EKF extremum seeking control application on the ANN model at 2600 motor rpm.

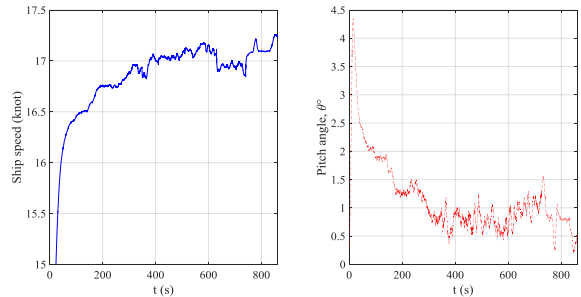


Figure 15. The craft's speed, knot, and pitch angle, θ° , are given by the time axes in consequence of the EKF extremum seeking control application on the ANN model at 2600 motor rpm.

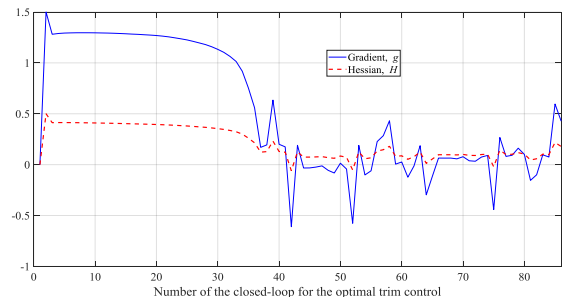


Figure 16. The gradient, g and Hessian, H are given by the time axes in consequence of the EKF extremum seeking control application on the ANN model at 2600 motor rpm.

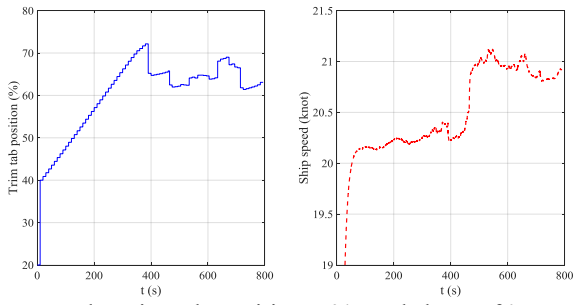


Figure 17. The trim tab positions, %, and the craft's speed, knot, are given by the time axes in consequence of the EKF extremum seeking control application on the ANN model at 3000 motor rpm.

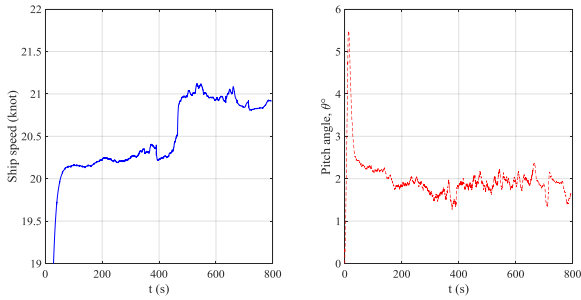


Figure 18. The craft's speed, knot, and pitch angle, θ° , are given by the time axes in consequence of the EKF extremum seeking control application on the ANN model at 3000 motor rpm.

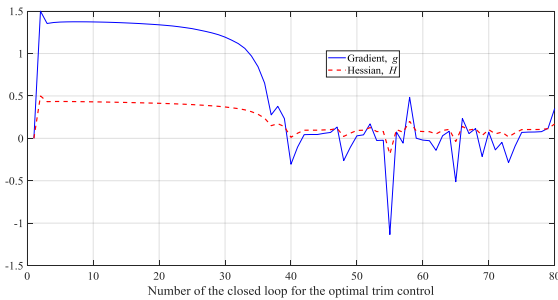


Figure 19. The gradient, g and Hessian, H are given by the time axes in consequence of the EKF extremum seeking control application on the ANN model at 3000 motor rpm.

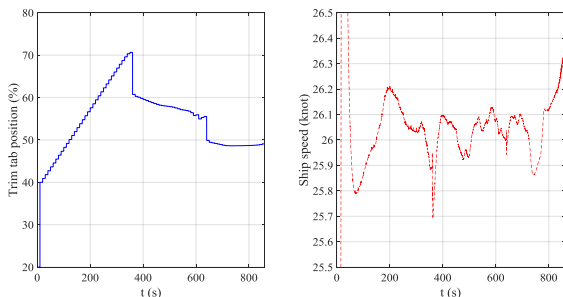


Figure 20. The trim tab positions, %, and the craft's speed, knot, are given by the time axes in consequence of the EKF extremum seeking control application on the ANN model at 3700 motor rpm.

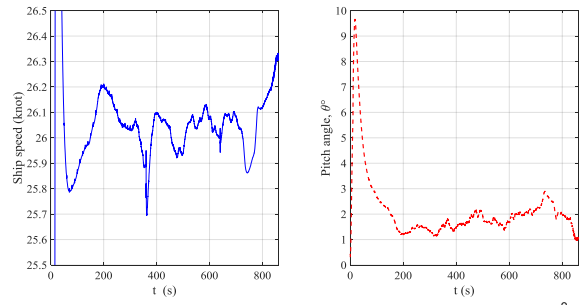


Figure 21. The craft's speed, knot, and pitch angle, θ° , are given by the time axes in consequence of the EKF extremum seeking control application on the ANN model at 3700 rpm motor rpm.

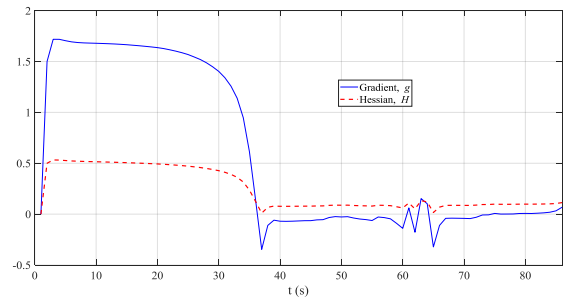


Figure 22. The gradient, g and Hessian, H are given by the time axes in consequence of the EKF extremum seeking control application on the ANN model at 3700 motor rpm.

5 CONCLUSIONS AND FUTURE WORK

To maintain the optimal trim angle for a high-speed craft using the trim tab, the interceptor, or the sterndrive propulsion systems, under changing environmental conditions provides an increment on its speed, energy efficiency, and well sight during a captain's driving.

To realize an automatic optimal trim control of a high-speed craft, a pair of interceptors and trim tabs were mounted on the craft. So, the sea trial data was obtained. A GPS and an AHRS were used to collect feedback data in changing sea conditions for system identification and to observe maximum effects. The GPS will be utilized as sole sensor for final prototype.

The EKF extremum seeking trim control was applied on the nonlinear coupled ANN model of the high-speed craft for three different motor rpm as 2600, 3000, and 3700 during changing dynamic conditions. The ANN model is based on variables such as pitch motion, θ° , heave acceleration, \ddot{z} , cruise speed, V , motor rpm, and the interceptor/trim tab systems' position, α .

As a result of these applications, the EKF extremum seeking control was lead to maintain the optimum

position of the trim tab systems's position, so the optimum speed values were obtained. Also, the pitch motions were nearly reduced because of the optimum trim condition. The most speed increase was occurred for the semi-planing running regime of the high-speed craft, while keeping optimum trim condition.

Although the nearly optimum trim condition was maintained with the EKF control, it was taken time to lead the optimum trim condition. Also, the control gain, K , needs to be tuned when motor power is changed. So, the EKF extremum seeking trim control could be used with the aid of an advanced tuning method. The improved optimal trim control will be implemented on sea trials. In the near future, the advanced trim control design studies and the experimental results will be presented in an upcoming paper.

ACKNOWLEDGEMENTS

Authors would like to thank I.T.U. Scientific Research Funds for partial support (project number: 37491) and The Republic of Turkey Ministry of Industry and Trade, 1507 - SME RDI (Research, Development & Innovation) Grant Programme for the support provided for the project numbered 7141282.

The author is also grateful to the University of Southampton for facilitating the research.

REFERENCES

Brown, R., Hwang, P. (1997) *Introduction to random signals and applied Kalman Filtering: with MATLAB exercises and solutions*. Wiley, 1997.

Brown, N., Schaefer, J. (2013) *Peak-seeking optimization of trim for reduced fuel consumption: flight-test results*. AIAA Guidance, Navigation, and Control (GNC) Conference, Boston, MA.

Cazenave, T.J.W. (2012) *Peak-seeking control of propulsion systems*. MSc. Thesis, School of Aerospace Engineering, Georgia Institute of Technology, USA.

Cotton, R.G., inventor. (2000). *Trim tab actuator for power boats*. US Patent. Patent No: 6,085,684.

Davis, D.R., inventors. (1993) *Automatic trim tab control for power boats*. US Patent. Patent No:5,263,432.

Davis, M.R., Watson, N.L., Holloway, D.S. (2004). *Measurement and prediction of wave loads on a high-speed catamaran fitted with active stern tabs*. Marine Structures, Vol. 17, pp. 503-535.

Day, A.H., Cooper, C. (2011). *An experimental study of interceptors for drag reduction on high-performance sailing yachts*. Ocean Engineering, Vol. 38, pp. 983-994.

Demuth, H.B., Beale, M.H., Hagan, M.T. (2013). *Neural Network Toolbox™*, Version 8.0.1, The MathWorks, Inc.

Ertogan, M., Wilson, P.A., Tayyar, G.T., Ertugrul, S. (2017) *Optimal trim control of a high-speed craft by trim tabs/interceptors Part I: Pitch and surge coupled dynamic modelling using sea trial data*. Ocean Engineering, Vol. 130, pp. 300-309.

Funami, Y., Watanabe, Y. inventors; Seisakusho, K.K.S. (1992) *Method of and apparatus for controlling the angle of trim of marine propulsion unit*. US Patent. Patent No: 5,118,315.

Grewal, M., Andrews, A. (2001) *Kalman Filtering: Theory and Practice Using MATLAB*. Wiley, 2001.

Hagan, M.T., Demuth, H.B., Beale, M.H., De Jesus, O. (2014). *Neural Network Design*. Martin Hagan, 2nd edition, ebook.

Karimi, M.H., Seif, M.S., Abbaspoor, M. (2013) *An experimental study of interceptor's effectiveness on hydrodynamic performance of high-speed planing craft*. Polish Maritime Research, 2(78), Vol. 20, pp. 21-29.

Krueger, W.R. inventor; Bombardier Motor Corporation of America, assignee. (2002) *Dynamic trim of a marine propulsion system*. US Patent. Patent No: 6,458,003 B1.

Kwang-Cheol S., Gopakumar, N., Atlar, M. (2013). *Experimental investigation of dynamic trim control devices in fast speed vessel*. J. Navig. Port Res., Vol. 37, No. 2, pp. 137-142.

Olofsson, N., inventor; Humphree AB, assignee. (2014). *Arrangement for dynamic control of running trim and list of a boat*. US Patent. Patent No: 8,622,012 B2.

Payne, P.R. (1990). *Planing and impacting plate forces at large trim angles*. Ocean Engng, Vol. 17, No. 3, pp. 201-233.

Ryan, J.J., Speyer, J.S. (2010) *Peak-seeking control using gradient and hessian estimates*. American Control Conference, 30 June-2 July 2010, Baltimore, MD, USA.

Ryan, J.J. (2012) *A method of extremum seeking control based on a time varying Kalman Filter and its application to formation flight*. PhD thesis, Aerospace Engineering, University of California, Los Angeles, USA.

Ryan, J.J., Speyer, J.L. (2013) *Systems and methods for peak-seeking control*. United States Patent, Patent No: US 8,447,443 B1, May 21, 2013.

Tsai, J.F., Hwang, J.L. (2004). *Study on the compound effects of interceptor with stern flap for two fast monohulls*. MTTTS/IEEE Techno-Ocean'04, Kobe, Japan, pp. 1023-1028.

Uenage, T., Hirano, Y., inventors; Kaisha, S.K.K., assignee. (1994) *Automatic trim controller for marine propulsion unit*. US Patent. Patent No: 5,366,393.